Available online at www.sciencedirect.com
ScienceDirect
Journal of Hazardous Materials 147 (2007) 871–882
Journal of Hazardous Materials
www.elsevier.com/locate/jhazmat

Incineration of a small particle of wet sewage sludge: A numerical comparison between two states of the surrounding atmosphere

Besma Khiari [a,b], Frederic Marias [b,*], Jean Vaxelaire [b], Fethi Zagrouba [c]

[a] *Centre des Recherches et Technologies de l'Energie, B.P. 95, 2050 Hammam-Lif, Tunisia*
[b] *Laboratoire de Thermique Energétique et Procédés, Université de Pau et des Pays de l'Adour, Rue Jules Ferry, B.P. 7511, 64075 Pau Cedex, France*
[c] *Institut Supérieur des Sciences et Technologies de l'Environnement, B.P. 95, 2050 Hammam-Lif, Tunisia*

Received 18 October 2006; received in revised form 23 January 2007; accepted 24 January 2007
Available online 30 January 2007

Abstract

The main goal of this paper is to elaborate a mathematical model that represents the physics and chemistry involved when a small particle of wet sewage sludge is incinerated. Compared to existing models, our study includes both drying and heterogenous combustion of the pyrloysis residue of the processed sludge. This model relies on the assumption of homogeneous composition and temperature for the particle under study. It includes drying, pyrolysis (controlled by a four successives steps reaction pathway) and combustion of the resulting char. The ability of the model is illustrated using it in two different process conditions (representing thermogravemetric analysis and fluidized bed conditions) in order to investigate the influence of the surrounding atmosphere. It is found, that fluidized bed conditions reduce the burnout time of a small particle by enhancing the rate at which heat is transferred to that particle. It is also shown that high heating rates enhance the tar yield.

Keywords: Pyrolysis; Incineration; Sludge; Modeling; Fluidized bed

1. Introduction

In the frame of sludge disposal trough incineration, fluidized bed reactors are known to offer high rates of destruction with low toxic gaseous emissions what is particularly true for nitrogen containing species (NO_x). Fluidized beds offer such possibility because they have excellent transfer properties and because they operate at a temperature lower than the one that may be encountered in other processes [1–3]. Although these devices have been operating for a long time, research is still required in order to improve the knowledge and the daily performances of these particular incinerators. Such improvements can be carried out by the use of simulators that represent the physical and chemical processes occurring within the furnace [4]. Our goal is to elaborate such simulators able to yield the working parameters (temperature of the post combustion, composition of the exhaust gas, etc.) given a set of operating parameters (sludge flow rate, mass flow rate of the fluidizing air, etc.). In some previous studies [5,6], we have shown the possibility to build such tools based on a five zone description of a hot fluidized bed. However these previous works were relying on the assumption of instantaneous drying and pyrolysis of the incoming waste, which we expect to be a coarse assumption. This is the reason why we have chosen to focus on the behaviour of a single particle of sludge, once it is placed in a given thermo-physical environement. Indeed, our present objective is to write a mathematical model, which represents the physical and chemical processes undergone by a particle submitted to heat at different rates. This model will be, in some further work, included within the general fluidized bed incinerator model.

Very few experimental and theoretical efforts have been made to analyze all the stages that sewage sludge may undergo during incineration (drying, devolatilization and char combustion) [7,8] and fewer again about its fluidized bed incineration [9]. Dealing with drying, Ogada and Werther [9] have shown that the time of drying increases with the diameter of the pellets and decreases with the rise in the temperature of the bed.

Devolatilization was extensively investigated for coal or biomass, but few authors have studied pyrolysis of wastes such as sewage sludge [3,10–12], and only some researchers con-

* Corresponding author. Tel.: +33 5 59 40 78 09; fax: +33 5 59 40 78 01.
E-mail address: frederic.marias@univ-pau.fr (F. Marias).

0304-3894/$ – see front matter © 2007 Elsevier B.V. All rights reserved.
doi:10.1016/j.jhazmat.2007.01.109

Nomenclature

a_w	water activity
A_i	Pre-exponential factor (s^{-1})
Ar_{sand}	Archimede number for sand particles
$C_{p_{sl}}$	heat capacity of sewage sludge ($J\,kg^{-1}\,K^{-1}$)
C_{p_∞}	heat capacity of air ($J\,kg^{-1}\,K^{-1}$)
$C_{p_w}^{liq}$	heat capacity of liquid water ($J\,kg^{-1}\,K^{-1}$)
C_i^s	mass concentration of species i at the surface of the particle ($kg\,m^{-3}$)
C_i^∞	mass concentration of species i in the surrounding gas ($kg\,m^{-3}$)
d_{sand}	diameter of sand particle (m)
E_1	activation energy ($J\,mol^{-1}$)
F_m	mass flow rate ($kg\,s^{-1}$)
$F_{m,w}^{bound,T}$	mass flow rate of bound water extracted from the particle at temperature T ($kg\,s^{-1}$)
$F_{m,w}^{free,T}$	mass flow rate of free water extracted from the particle at temperature T ($kg\,s^{-1}$)
h_T	convective heat transfer coefficient ($W\,m^2\,K^{-1}$)
h_T^*	overall heat transfer coefficient ($W\,m^2\,K^{-1}$)
H_p	particle enthalpy (J)
ΔH_w^{des}	enthalpy of water desorption ($J\,kg^{-1}$)
ΔH_w^{vap}	enthalpy of water vaporization ($J\,kg^{-1}$)
k_i	kinetic constant of pyrolysis reactions (s^{-1})
k_m	mass transfer coefficient ($m\,s^{-1}$)
k_s	kinetic constant of char combustion reaction ($m\,s^{-1}$)
m	mass (kg)
$\dot{m}_{vol}$	production rate of volatiles (primary or secondary) ($kg\,s^{-1}$)
m_{OM}^0	initial mass of organic matter in the particle (kg)
M_w	molar weight of liquid water ($kg\,mol^{-1}$)
Nu	Nusselt number
P_w^{sat}	vapor pressure of water (Pa)
Q^{comb}	flow rate of heat due to char combustion (W)
Q^{dr}	flow rate of heat due to drying (W)
Q^{ext}	heat flow rate transferred between the particle and its surrounding atmosphere (W)
Q^{react}	flow rate of heat due to reaction (W)
r	particle radius (m)
R	universal gas constant ($J\,mol^{-1}\,K^{-1}$)
$\Delta_r H_C$	heat of pure carbon combustion ($J\,kg^{-1}$)
$\Delta_r H_i$	enthalpy of pyrolysis of reaction i ($J\,kg^{-1}$)
Sc	Schmidt number
Sh	Sherwood number
T	local temperature (K)
T_{film}	average temperature between the air temperature and the particle temperature (K)
T_p	particle temperature (K)
$T_{reactor}$	reactor temperature (K)
T_{ref}	reference temperature (K)
T_∞	temperature of the surrounding atmosphere (K)
T^{eb}	water ebullition temperature (K)
T_∞^{in}	inlet air temperature (K)
U_{mf}	fluidization velocity at incipient conditions ($m\,s^{-1}$)
W	water content (dry basis)
X	normalized mass; (m_i/m_{OM}^0)
$y_{O_2}^\infty$	oxygen mass fraction in the gas surrounding the particle (%)

Greek letters

β	molar weight ratio of carbon to oxygen
ε	particle emissivity
ε_{mf}	porosity of the bed at incipient fluidization
λ_∞	thermal conductivity of air ($W\,m^{-1}\,K^{-1}$)
Λ	stoeichiometric coefficient in Eq. (12)
μ_∞	air dynamic viscosity (Pa s)
ρ_p	particle density ($kg\,m^{-3}$)
ρ_∞	air density ($kg\,m^{-3}$)
ρ_w^{sat}	water mass concentration at the surface of the particle in saturated air conditions ($kg\,m^{-3}$)
ρ_w^{vap}	water mass concentration at the surface of the particle in non-saturated conditions ($kg\,m^{-3}$)
ρ_w^∞	water mass concentration in surrounding atmosphere ($kg\,m^{-3}$)
σ	Stefan–Boltzmann constant ($W\,m^{-2}\,K^{-4}$)

Subscripts

ch	char
I	intermediate
OM	organic matter
vol1	primary volatiles
vol2	secondary volatiles
w	water

Superscripts

bound	bound water
comb	combustion
free	free water
pyr1	primary pyrolysis
pyr2	secondary pyrolysis

sidered it as the second step in the gasification or incineration process [7,13]. According to the temperature and the heating rate, the proportion of the pyrolysis products is different [14,15]. Kaminsky and Kummer [16] showed that the proportion of gases of digested sludge pyrolysis increases from 22.7 to 40.8% when temperature rises from 893 to 1023 K whereas that of tar decreases from 40.1 to 21.1%. Similar tendencies were reported for flocculated sludge incineration in TGA (thermogravimetric analysis) conditions in the range of 300–900 K by Chu et al. [17]. An important issue in the modeling of the devolatilisation step is the reaction pathway. Research on this problem has resulted in three main classes of models: the first one is based on reactions in parallel [10,17,18–20], the second one relies upon successive mechanisms [21–23], whereas the third is obtained according to the distribution of activation energy [12,24].

The combustion of char takes place throughout the particle [1,2,9] or at its surface [5,25] according to the authors and to the models proposed. Marias et al. [5] proposed an approach that considers that the mass transfer within the particle limits oxygen penetration forcing the burn out to occur at its surface and leading to a change in its diameter. The char shrinks at constant density under external mass transfer control during oxidation. The rate of reaction of a particle is then proportional to its external surface area and to a mass transfer coefficient, itself a function of particle diameter.

Given this information a mathematical model relating the drying, pyrolysis and combustion phenomena that a small particle of wet sludge undergoes once it is heated, has been written. This is the scope of the second section of the paper. Once the main assumptions have been laid down, the equations allowing for the computation of the relevant data are derived.

As stated at the beginning of this introduction, our objective is to include this model of a single particle within a more general model of a fluidized bed incinerator. Such an inclusion is not within the scope of this paper. However, by itself, this model allows for a better comprehension of the impact of fluidization on the incineration of a particle of sludge and this is what we want to show here. Thus, in the third section, some numerical experiments are performed that compare the evolution of a particle in two different situations: the first one represents the conditions prevailing within a thermo balance while the second one is related to fluidized bed processing. These two experiments exhibit different properties particularly for the burn out time and the tar yield.

2. Numerical model

The model presented in this study aims to describe the evolution of wet sewage sludge during its incineration. The three main steps occuring during this process are drying, pyrolysis and heteregeneous combustion of the pyrolysis residue (when neglecting homogeneous combustion of the volatiles). These various processes are elucidated on the basis of the history of an isolated particle of a wet sewage sludge suspended in an upward air flow within a cylindrical reactor. As the final aim of this study is to upgrade the current treatment of the process of incineration in bubbling fluidized bed reactors, and in order to limit the overall central processing unit (CPU) requirements, we had to reduce its complexity: the particle was assumed to be homogeneous and internal transfers issues were not taken into account.

2.1. Main simplifying hypothesis

The main assumptions of the model are listed below:

- The raw sewage sludge is considered as a spherical particle. It is considered as a homogeneous medium (no attention is paid to internal transports).
- The particle is composed of water, organic matter (volatiles, intermediate and char) and ash.
- Only the particle is considered: further reactions of pyrolysis gas products are not accounted for.
- External mass transfer of the volatiles released during the pyrolysis step, is neglected. Their release from the particle is entirely controlled by their rate of production.
- The inorganic fraction is supposed to be chemically inert; its mass is therefore constant with respect to time.
- The atmosphere surrounding the particle is assumed to be homogeneous in composition and temperature.
- Water within the particle is divided in two categories: free water (not influenced by solids) and bound water. The repartition between theses two types of water is fixed by sorption isotherms data.
- The particle size is assumed to change with the departure of free water and with the combustion of char, whereas the density is assumed to vary with the volatiles departure as well as with the bound water leaving.

2.2. Energy balance

The characteristic kinetics of the different phases encountered during the incineration depend strongly on the particle temperature (T_p). It is therefore important to write the energy balance which allows for the computation of its temperature. This balance must take into account the external heat transfer to the particle (Q^{ext}) which is the sum of a convective heat flux, considered between the particle and the surrounding gas, and a radiative term, exchanged between the particle and the reactor walls; its expression is given by:

$$Q^{ext} = 4\pi r^2(h_T(T_\infty - T_p) + \sigma\varepsilon(T^4_{reactor} - T^4_p)) \quad (1)$$

where r is the particle radius, h_T the convection heat transfer coefficient, ε the particle emissivity (fixed to 0.75 in this study), σ the Stephan–Boltzmann constant, T_∞ and $T_{reactor}$ the temperature of the surrounding gaseous atmosphere and of the reactor wall, respectively.

Some other terms must be included in this equation. They are relative to the energy of pyrolysis and combustion reactions Q^{react} on one hand, and to the water departure during drying Q^{dr} on the other hand. The expressions of these quantities are evaluated later in this paper.

Finally, the energy balance brings out the particle temperature by writing:

$$\frac{dH_p}{dt} = Q^{ext} - Q^{dr} + Q^{react} \quad (2)$$

where H_p is the particle enthalpy, that is written by:

$$H_p = (m_w C^{liq}_{p_w} + m_s C^{liq}_{p_{sl}})(T_p - T_{ref}) \quad (3)$$

In this expression, T_{ref} is reference temperature and m_s is the total solid mass of the particle, which is expressed by:

$$m_s = m_{OM} + m_I + m_{ch} + m_{ash} \quad (4)$$

$C^{liq}_{p_w}$ is heat capacity of the liquid water, the expression of which is given later and $C^{liq}_{p_{sl}}$ is that of the solid matrix, which is supposed to be independant of its composition. Its value is fixed to $1350\,J\,kg^{-1}\,K^{-1}$ [26].

Table 1
Water mass flux expressions for free and bound water during evaporation and bullition

	Free water	Bound water
$T_p < T^{eb}$	$F_{m,w}^{free,T_p} = 4\pi r^2 k_m(\rho_w^{sat} - \rho_w^{\infty})$	$F_{m,w}^{bound,T_p} = 4\pi r^2 k_m(\rho_w^{vap} - \rho_w^{\infty})$
$T_p = T^{eb}$	$F_{m,w}^{free,T_{eb}} = \dfrac{Q^{ext} + Q^{react}}{\Delta H_w^{vap}}$	$F_{m,w}^{bound,T_{eb}} = \dfrac{Q^{ext} + Q^{react}}{\Delta H_w^{vap} + \Delta H_w^{des}}$

2.3. Heat and mass fluxes modelling

2.3.1. Drying

Given a proximate analysis of a wet sludge, water content can be as high as 90% of its total weight. Consequently, drying generally appears as the first stage in the incineration operation. The particle temperature can range from ambient to water ebullition temperature, during this dewatering. When the particle temperature is lower than the ebullition temperature of water, the drying is controlled by the difference in water concentration between the material surface and the surrounding ambiant air. When the ebullition temperature is reached, evaporation is assumed to happen under isothermal conditions. All the incoming thermal flux (Q^{ext} and Q^{react}) is consumed for water vaporization. These two situations are described with the help of the mathematical formulation given in Table 1 in terms of water mass flux leaving the particle $F_{m,w}$ (kg s^{-1}). Two cases are presented depending whether free or bound water is removed. When drying is controlled by mass transfer, the water concentration at the surface of the particle is considered to be equal to the saturation concentration of free water (ρ_w^{sat}) whereas it takes a lower value (ρ_w^{vap}) for bound water due to solid–liquid interactions. This value can be calculated with regards to the sorption isotherm data:

$$\rho_w^{vap} = a_w \rho_w^{sat} \tag{5}$$

where a_w is water activity.

During ebullition, the enthalpy of desorption has to be considered so as to describe the bound water removing. The transition between free and bound water is defined according to isotherm sorption data (which represents the sludge water content in function of of the water activity) [27]: when a_w is lower than one, water is bound.

The heat flow rate relative to water removal is equal to $F_{m,w}\Delta H_w^{vap}(T_p)$, when the drying is controlled by mass transfer. During the ebullition phase in drying, the way the mass flow rate is computed leads to a constant temperature of the particle.

2.3.2. Pyrolysis

The reactional pathway based on four consecutive-parallel reactions with the formation of an intermediate compound was considered to model the pyrolysis step because it was successfully applied through the literature relative to sewage sludge [21–23].

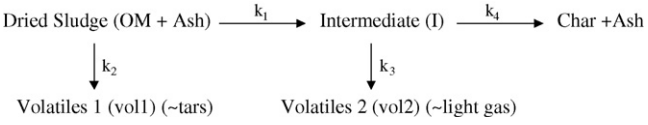

Assuming that the particle size remains constant during pyrolysis, the mass flow rates of the different compounds for the primary and secondary pyrolysis are expressed as:

- Produced primary volatile mass flow rate:

$$F_{m,vol1}^{pyr1} = k_1 m_{OM}^0 X_{OM}^{n_1} \tag{6}$$

- Produced intermediate mass flow rate:

$$F_{m,I}^{pyr1} = k_2 m_{OM}^0 X_{OM}^{n_2} \tag{7}$$

- Produced secondary volatile mass flow rate:

$$F_{m,vol2}^{pyr2} = k_3 m_{OM}^0 X_I^{n_3} \tag{8}$$

- Produced char mass flow rate:

$$F_{m,ch}^{pyr2} = k_4 m_{OM}^0 X_I^{n_4} \tag{9}$$

In these expressions k_i is the kinetic constant of pyrolysis reactions, n_i is the reaction order, m_{OM}^0 is the initial organic matter mass and X_i is the normalized mass of compound i ($X_i = m_i/m_{OM}^0$).

The heat flow rates relative to these reactions can be calculated by the following relationships:

- for primary pyrolysis:

$$Q^{pyr1} = F_{m,vol1}^{pyr1}\Delta_r H_1 + F_{m,I}^{pyr1}\Delta_r H_2 \tag{10}$$

- for secondary pyrolysis:

$$Q^{pyr2} = F_{m,vol2}^{pyr2}\Delta_r H_3 + F_{m,ch}^{pyr2}\Delta_r H_4 \tag{11}$$

where $\Delta_r H_i$ represents the heat of the considered reactions.

2.3.3. Combustion of char

As mentionned in many works, the char combustion kinetics are significantly controlled by external mass transfer. Combination of external transfer and reaction kinetics allows calculating the mass flow rate of consumed char. The following expression of char mass flow rate is that used in works of Marias et al. [5]:

$$F_{m,ch}^{comb} = 4\pi r^2 \rho_\infty y_{O_2}^{\infty}\left(\frac{\beta k_s k_m}{\Lambda k_s + k_m}\right) \tag{12}$$

where β is molar weight ratio of carbon by oxygen, $y_{O_2}^{\infty}$ is the oxygen mass fraction in the surrounding air and ρ_∞ is the air density. k_m is the mass transfer coefficient and k_s is the kinetic constant of the char combustion. The expressions of these two last quantities are given later in this paper. Λ is the stoeichiometric coefficient relative to the following chemical reaction:

$$C + \Lambda O_2 \rightarrow (2 - 2\Lambda)CO + (2\Lambda - 1)CO_2 \quad \text{with } \Lambda = 0.87$$

Heat flow rate associated to this char combustion can be written as:

$$Q^{comb} = F_{m,ch}^{comb}\Delta_r H_C \tag{13}$$

where $\Delta_r H_C$ is the enthalpy of pure carbon combustion.

Table 2
Water properties

Parameter of water	Expression or value
Water pressure at saturation (Pa)	$P_w^{sat} = \exp\left(73.65 - \frac{7258.2}{T_p} - 7.3\ln(T_p) + 4.16\times10^{-6}T_p^2\right)$
Water mass concentration at the surface of the particle in saturated air conditions (kg m^{-3})	$\rho_w^{sat} = \frac{P_w^{sat}M_w}{RT_p}$ with $M\omega$ the molar weight of water
Water activity	$a_w = 1 - \exp(-5.85T_p^{0.442}W^{14.23T^{-0.3953}})$ with W the sludge water content (dry basis)
Enthalpy of vaporization (J kg^{-1})	$\Delta H_w^{vap} = 28.92\times10^5\left(1-\frac{T_p}{647.13}\right)^{0.32-0.212(T_p/647.13)+0.26(T_p/647.13)^2}$
Enthalpy of desorption (J kg^{-1})	$\Delta H_w^{des} = \exp(13.71 - 31.90W)$
Heat capacity of liquid water (J kg^{-1} K)	$C_{pw}^{liq} = 15353.89 - 116.12T_p + 0.45T_p^2 - 7.84\times10^{-4}T_p^3 + 5.20\times10^{-7}T_p^4$
Diffusivity of water in air (m^2 s^{-1})	2.88×10^{-5}

2.4. Mass balances

Mass balances are derived to follow the mass evolution of the different compounds (water, organic matter, intermediate, char and ash) over time:

$$\frac{dm_w}{dt} = -F_{m,w}^{free,T} - F_{m,w}^{free,T^{eb}} - F_{m,w}^{bound,T} - F_{m,w}^{bound,T^{eb}} \quad (14)$$

$$\frac{dm_{OM}}{dt} = -F_{m,vol1}^{pyr1} - F_{m,I}^{pyr1} \quad (15)$$

$$\frac{dm_I}{dt} = F_{m,I}^{pyr1} - F_{m,vol2}^{pyr2} - F_{m,ch}^{pyr2} \quad (16)$$

$$\frac{dm_{ch}}{dt} = F_{m,ch}^{pyr2} - F_{m,ch}^{comb} \quad (17)$$

$$\frac{dm_{ash}}{dt} = 0 \quad (18)$$

The global mass balance allows for the computation of both the particle radius and of its density. The evolution of the particle radius is induced by the free water departure and the combustion of char, in accordance with the following relationship:

$$4\pi r^2\rho_p\frac{dr}{dt} = \frac{dm_w^{free}}{dt} + \frac{dm_{ch}}{dt} \quad (19)$$

The particle density (ρ_p) is modified when removing the bound water and when consuming organic material or intermediate:

$$\frac{4}{3}\pi r^3\frac{d\rho_p}{dt} = \frac{dm_w^{bound}}{dt} + \frac{dm_{OM}}{dt} + \frac{dm_I}{dt} \quad (20)$$

2.5. Model parameters

The different properties and parameters used in the model are presented in this section. Table 2 deals with the parameters relative to water properties. The relationships used to compute the vapor pressure of water (P_w^{sat}), the enthalpy of water desorption (ΔH_w^{vap}) and the heat capacity of liquid water (C_{pw}^{liq}) are issued from the PROSIM Plus Thermodynamic Library. Desorption data such as water activity (a_w) and enthalpy of water desorption (ΔH_w^{des}) are derived according to experimental results obtained on activated sludges [27]. The water diffusivity is considered as constant on the range of temperature corresponding to drying (i.e. 293–373 K). Its value at 313 K is issued from Tosun [28].

The physical properties relative to surrounding gas (which is assumed to be air) are computed by using relationships drawn from PROSIM. In the vicinity of the particle, the temperature is different from the gas temperature T_∞ and of particle temperature T_p. These properties (reported in Table 3) were therefore calculated within a thin film considered between the particle and its surrounding gas. This interface temperature, indicated in Table 3 by T_{film}, is an average between the particle and air temperatures. The diffusivity of oxygen in air is calculated with respect to the temperature by the relationships proposed by Reid et al. [29]. Relative humidity of incoming air is fixed arbitrarily in our case to 40%.

Two sludges (B1 and B2) presenting different sets of kinetics parameters for pyrolysis have been considered according to Chen and Jeyaseelan [22] results (Table 4). The kinectic constants of each reaction are from an Arrhenius type relationship:

$$k_i = A_i\exp\left(\frac{-E_i}{RT_p}\right) \quad (21)$$

where A_i is the pre-exponential factor, E_i is the activation energy, R is the universal gas constant and T_p is the particle temperature.

Table 3
Air properties

Parameter of air	Expression or value
Dynamic viscosity (Pa s)	$\mu_\infty = \frac{1.42\times10^{-6}T_{film}^{0.5039}}{1+(108.3/T_{film})}$
Density (kg m^{-3})	$\rho_\infty = \frac{345.8}{T_{film}}$
Heat conductivity (W m^{-1} K^{-1})	$\lambda_\infty = \frac{3.1410^{-4}T_{film}^{0.78}}{1-(0.71/T_{film})+(2121.7/T_{film}^2)}$
Heat capacity of air (J kg^{-1} K)	$C_{p\infty} = 1608.78 + 521.67\left(\frac{(3012/T_{film})}{\sinh(3012/T_{film})}\right)^2 + 421.11\left(\frac{(1484/T_{film})}{\cosh(1484/T_{film})}\right)^2$
Relative humidity (%)	40

Table 4
Kinetic parameters of pyrolysis reaction [22]

Reaction	Frequency factor, A_i (s^{-1})		Energy, E_i ($J\,mol^{-1}$)		n_i	$\Delta_r H_i$ ($J\,kg^{-1}$)
	B1	B2	B1	B2		
1	148.3	1101	5.27×10^4	6×10^4	1	0
2	27,337	558.9	7.32×10^4	5×10^4	1	0
3	6.9×10^{12}	61.50	20.5×10^4	6.34×10^4	1	0
4	2596	61.13	7.58×10^4	7.08×10^4	1	0

Pyrolysis of sludge is often considered as endothermic by some authors while some others assume it to be exothermic. For our purposes, it has been assumed to be athermic. This leads to nil value for the enthapies of pyrolysis reactions.

The relationship proposed by Sriramulu et al. [30] was considered to bring out the kinetic constant of the char combustion (k_s):

$$k_s = 595 T_p \exp\left(\frac{-149220}{R T_p}\right) \quad (22)$$

External heat and mass transfer coefficients around an r-radius spherical particle are deduced from the correlations presented in Table 5. Two different cases are considered according to whether the particle is surrounded by stagnant gas or is in fluidized bed conditions.

The first situation is characterized by Nusselt and Sherwood numbers both equal to two, whereas the fluidized bed condition is described by correlations proposed by Prins [31].

In these correlations ε_{mf} is the porosity of the bed at incipient fluidization (fixed to 0.41) and U_{mf} is the incipient fluidization velocity, the expression of which is given by Thonglip et al. [32]:

$$U_{mf} = \frac{\mu_\infty(\sqrt{31.6^2 + 0.0425 Ar_{sand}} - 31.6)}{\rho_\infty d_{sand}} \quad (23)$$

where Ar_{sand} is the Archimede number for sand particles. The diameter of sand particles (d_{sand}) is fixed to 1 mm in this study.It is important to note that the overall transfer coefficient (h_T^*) cannot be directly compared to the convection coefficient h_T because, because the relationships used for fluidized bed conditions (Table 5) includes both convection and radiation phenomena. This aspect is taking into account in the model by neglecting the radiation term in the expression of Q^{ext} (Eq. (1)).

2.6. Model validation

In order to validate the above described model, the different pyrolysis by-products mass profiles during the devolatilization of a pre-dried sludge were compared to experimental and numerical results reported by Chen and Jeyaseelan [22]. This work was selected because it offers a complete set of operating data and of kinetics parameters.

It was found that, for a heating rate of $0.25\,K\,s^{-1}$, the model developed, as far as only devolatilization is concerned, was in excellent agreement with their experimental data. The two graphs are confounded point by point which is the reason why the curves of comparison are not presented here.

The Biot's number ($2rh_T/\lambda_{sl}$) was calculated to see how far the assumption of homogenous particle is true. For this computation the sludge thermal conductivity (λ_{sl}) was fixed to $0.18\,W\,m^{-1}\,K^{-1}$ according to experimental data carried out on sewage sludge [33]. Biot's numbers ranging from 1.27 and 5.09 for fluidized bed and between 0.28 and 0.76 for stagnant bed were obtained. The hypothesis is well verified for stagnant bed, but can be rather critical for fluidized bed. However, in this last case, the Biot's number was calculated with respect to h_T^* which integrates both phenomena: convection and radiation. Consequently, as it remains lower than 10 we can consider the particle as a homogeneous medium and neglect internal thermal transfers.

3. Results and discussion

All following calculations treat spherical particles of sewage sludge (B1 and B2) with an initial temperature of 293 K at 1 atm, incinerated in ambiant air conditions (21 vol% O_2). The particle initial radius was 2 mm. It contains 60% of water and the dry mass is constituted by 65.4% of organic matter. The density of the dry sludge was fixed to $1200\,kg\,m^{-3}$ according to Chen and Jeyaseelan [22] data.

Table 5
Correlations used for transfer coefficients calculation

Operating conditions	Correlation
Stagnant gas (TGA)	$Sh = Nu = 2$
Fluidized bed [31]	$h_T^* = \frac{\lambda_\infty (3.539(2r/d_{sand})^{-0.257})(0.844 + 0.0756(T_{film}/273)) Ar_{sand}^n}{2r}$ with $n = 0.105\left(\frac{2r}{d_{sand}}\right)^{0.082}$, d_{sand} sand particle diameter (fixed to 1 mm) and Ar_{sand} the Archimede number relative to sand particle
	$k_m = \frac{U_{mf}}{\varepsilon_{mf}} Sc^{-2/3}\left(\frac{\rho_\infty}{\mu_\infty}\frac{U_{mf} d_{sand}}{(1-\varepsilon_{mf})}\right)^{-n'}\left(0.105 + 1.505\left(\frac{2r}{d_{sand}}\right)^{-1.05}\right)$ with $n' = 0.35 + 0.29\left(\frac{2r}{d_{sand}}\right)^{-0.5}$ and Sc the Schmidt number

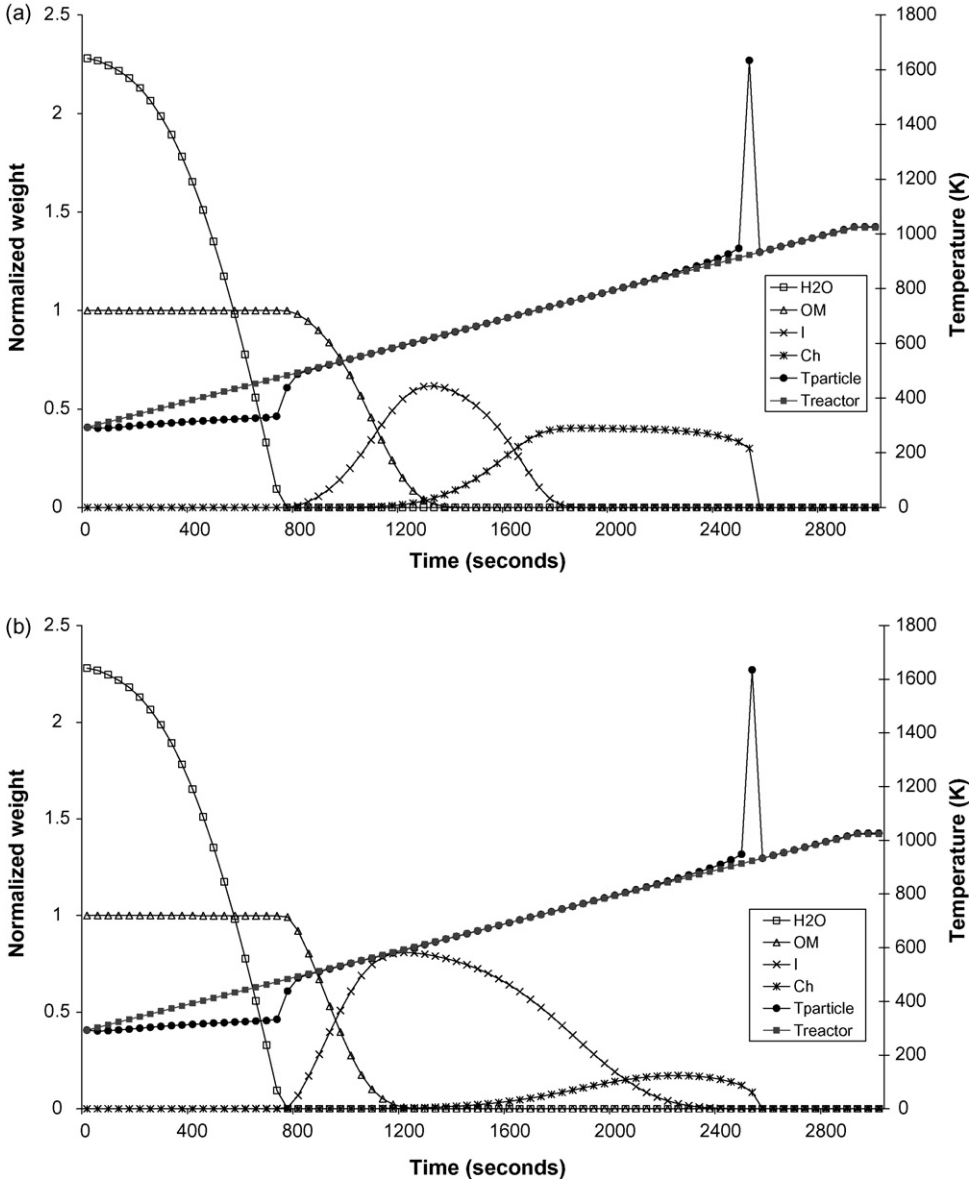

Fig. 1. Temperatures and incineration by-product mass fractions (a) sludge B1; (b) sludge B2. Operating conditions: stagnant atmosphere, 15 K min^{-1} heating rate and $T_\infty = T_{\text{reactor}}$.

In the first simulations, the case of a single particle surrounded by a stagnant atmosphere (the Nusselt and the Sherwood numbers were taken equal to 2) was considered to approximate TGA conditions. Then, the fluidized bed conditions were studied. The objective of these simulations is to follow the different mass profiles (water, organic matter, intermediate and char) and the evolution of temperature as well as the impact of the transfers on the operation of incineration.

3.1. Stagnant air

In this section, two configurations will be discussed. The first one corresponds to conditions which can be assumed to represent the thermogravimetry conditions. It considers a heating rate equal to 15 K min^{-1}. The second one is a more fictive situation, in which the heating rate corresponds to fluidized bed conditions (HR = 1000 K min^{-1}) but with transfer coefficients calculated for stagnant atmosphere. This approach aims to highlight the importance of the transfer phenomena in fluidized bed reactors.

3.1.1. 15 K min^{-1} heating rate

This situation is depicted in Fig. 1(a) for sludge B1 and 1.b for sludge B2. For this simulation, the convection heat coefficient (h_T) ranged between 12.8 and 53.6 W m^2 K^{-1}, and the mass transfer coefficients (k_m) varied from 0.01 and 0.13 m s^{-1}. The whole process lasts approximately 2600 s for both sludges and includes water removal, devolatilisation and char combustion. The drying phase lasts 750 s for B1 and B2, after which pyrolysis takes place at a temperature that coincides with that of walls. The devolatilization proceeds during approximately 1600 s (approximatively 3/5 of the whole process duration) for B2 and 1000 s for B1. Primary and secondary pyrolysis release

comparable amounts of volatiles (31.9 and 27.7%, respectively) for B1, whereas for sludge B2, the secondary pyrolysis releases more gas volatiles since its reduced mass is about four times greater (64.3%) than that of primary volatiles (16.5%). These values have been computed after integration with respect to time of the produced mass flow rates $F^{\mathrm{pyr1}}_{\mathrm{m,vol1}}$ and $F^{\mathrm{pyr2}}_{\mathrm{m,vol2}}$, which gives respectively:

$$m_{\mathrm{vol1}} = \int_1^{\infty} k_1 m^0_{\mathrm{OM}} X_{\mathrm{OM}}\, \mathrm{d}t \tag{24}$$

and

$$m_{\mathrm{vol2}} = \int_0^{\infty} k_3 m^0_{\mathrm{OM}} X_{\mathrm{I}}\, \mathrm{d}t \tag{25}$$

A comparison of the kinetic parameters of the two sludges confirms this report. One remarks that the value of the activation energy E_3 of the reaction which gives the secondary volatiles is lower in B2, which implies that reaction 3 progresses more rapidly and gives a larger amount of secondary gases. The reactions that give the intermediate compound and the char have also low activation energies for B2, which however has higher E_1 compared to B1. This corroborates the fact that B2 gives lower quantities of primary volatiles to the profit of the secondary ones.

The temperature at which the char begins to be produced is about 50 K higher for B1 than for B2. For both sludges, the peak in particle temperature observed around 1635 K corresponds to the disparition of char (final decrease in the radius of the particle).

3.1.2. 1000 K min^{-1} heating rate

Fig. 2a and b represents the evolution of the contents of the particle at a higher heating rate when $T_\infty = T_{\mathrm{reactor}}$ for B1 and

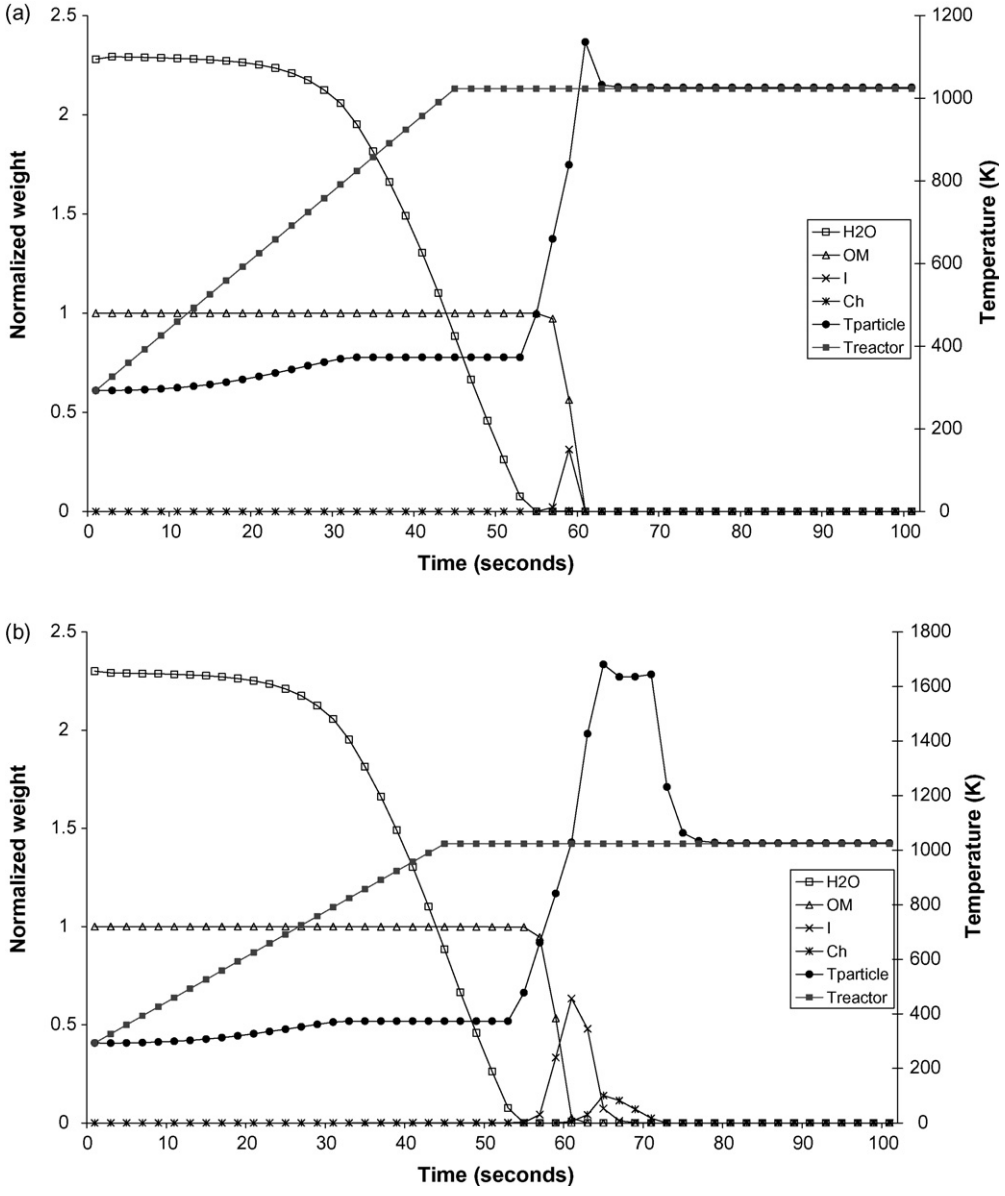

Fig. 2. Temperatures and incineration by-product mass fractions (a) sludge B1; (b) sludge B2. Operating conditions: stagnant atmosphere, 1000 K min^{-1} heating rate and $T_\infty = T_{\mathrm{reactor}}$.

B2. They logically show that the process of incineration lasts less time for higher heating rates: the incineration is completed in 80 s for B2 (65 s for B1) for a heating rate of 1000 K min^{-1} whereas it was achieved in about 2600 s for a heating rate of 15 K min^{-1} (Figs. 1 and 2). From these figures, one can see that drying phase lasts more than 3/4 of the whole duration of incineration process for the highest heating rate against less than the third (28%) for the lower one. During water removal, the whole of the provided energy is used for the evaporation of water. In this phase, the difference in temperature between the particle and the reactor is about 140 K when the heating rate is low, against 650 K for the higher one. A remark can be emitted here, concerning the fact that Ogada and Werther [9] reported that pyrolysis started before drying has ended. This is due to the fact that these authors have taken into account a drying front inside the sludge. In our case the small size of the sludge particle as well as the assumption of homogeneity do not make it possible to highlight this phenomenon.

The particle temperature increases rapidly as soon as drying is finished, and coincides with the reactor's temperature when primary pyrolysis is started. Next, it increases sharply with the combustion of char. The peak is more significant for B2 with high and low heating rates. In the case of sludge B1, the high value (1635 K) is observed only at low heating rate. Indeed, when submitted to the heating rate of 1000 K min^{-1}, the maximal temperature for the sludge B1 reaches 1135 K, due to the fact that the small quantity of the produced char is burnt out, as soon as it is formed. However, for both sludges the temperature drops instantaneously to the reactor temperature when all char is consumed. Infact, ashes are the only particle residues from

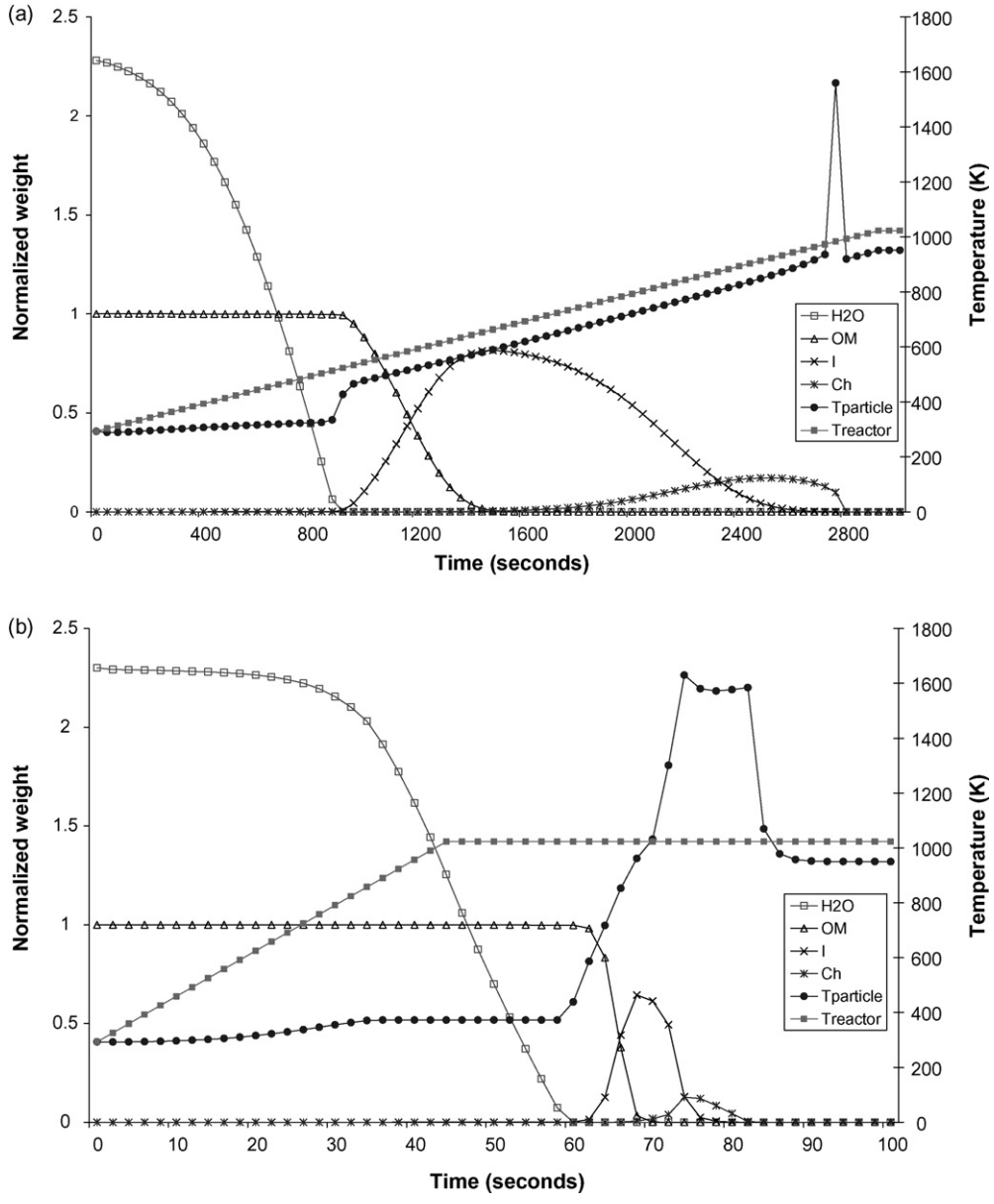

Fig. 3. Temperatures and incineration by-product mass fractions of sludge B2. Operating conditions: stagnant atmosphere, $T_\infty = (T_{reactor} + T_\infty^{in})/2$ and (a) 15 K min^{-1} heating rate; (b) 1000 K min^{-1} heating rate.

combustion and their temperature corresponds to that of the surrounding atmosphere, i.e. reactor temperature. As for the yields of the different by-products, one can see that the shape of the profiles depends on the heating rate. The maximal yield fraction of the intermediate compound in B2 is about 80% and that of char almost 17.2% in the low heating rate process against 63.4 and 14%, respectively, for the higher heating rate (Figs. 1b and 2b). This means that during pyrolysis more primary volatile gases are generated for higher heating rates. Computations show that primary volatiles fraction has almost doubled with increasing heating rates (from 16.5 to 31.8% for 15 and 1000 K min^{-1}, respectively). The ratio m_{vol1}/m_{vol2} was found to be 25.6% for the low heating rate and 71.8% for the higher one. This means that we form more tars than light gases in the second case, and that thermogravimetry conditions are more suitable to get larger quantities of light gases such as hydrogen or methane (when pyrolysis operation is carried out).

In fact, the surrounding gas temperature evolves differently from walls' reactor temperature during time [34]. Indeed, the residence time of the incoming gas is not long enough for it to reach the reactor temperature. A possible simulation compromise is to consider an average temperature between the initial temperature of incoming air and reactor temperature. Fig. 3a and b represents this situation for sludge B2. It arises from these figures that not only the final particle temperature is lower than that of the reactor, but that it is also lower than the particle temperature at every location in the case where the surrounding gas is estimated to be at the same temperature as the one of the reactor. This results in longer times for the different stages to occur (drying, devolatilization and char combustion), which indicates the importance of convection heat transfers at such temperatures.

Water as well as the pyrolysis by-products are released later for different heating rates, but have the same shape, the same yields and the same duration for the low heating rates. For the high heating rate, the curve shape changes due to the variation of the lifetime of each product. The drying phase lasts longer because the water mass concentration at saturation at particle surface is lower. The devolatilization and combustion processes are slowed down since their kinetics are governed by Arrhenius' law.

From these different sets of simulations, one can note that it is important to know air conditions (velocity, temperature, etc.) around the sample. This shows the interest in using computational fluid dynamics (CFD) in order to correctly interprete experiments carried out by TGA [34].

3.2. Fluidized bed conditions

In fluidized bed reactors, higher transfer coefficients are expected (heat and mass transfer coefficients range from 58 to 205 W m^2 K^{-1} and from 0.1 to 0.3 m s^{-1}, respectively). Their influence on the overall process of incineration is depicted in Fig. 4. This figure has to be compared to Fig. 2b where the same heating rate was used but with transfer coefficients estimated from stagnant conditions. In both cases, the compound profiles over time have almost the same shape. Nevertheless, the more efficient transfers lead to a faster drying, which in turn leads to an earlier pyrolysis (10 s). The maximal temperature is higher by about 950 K in fluidized bed conditions compared to that observed in stagnant atmosphere for the same reactor heating rate. This difference of temperature causes a shorter period for the char to burn out.

An analysis can also be made concerning the comparison of the yields of char which is higher in fluidized bed conditions by about 12%. This means that the relative ratio of primary volatiles to secondary ones was shifted from the 71.8% obtained in stagnant air. Calculations in deed brought out that in this case the ratio m_{vol1}/m_{vol2} is 81.1%, which confirms that fluidized bed conditions favor the formation of tars rather than light gases,

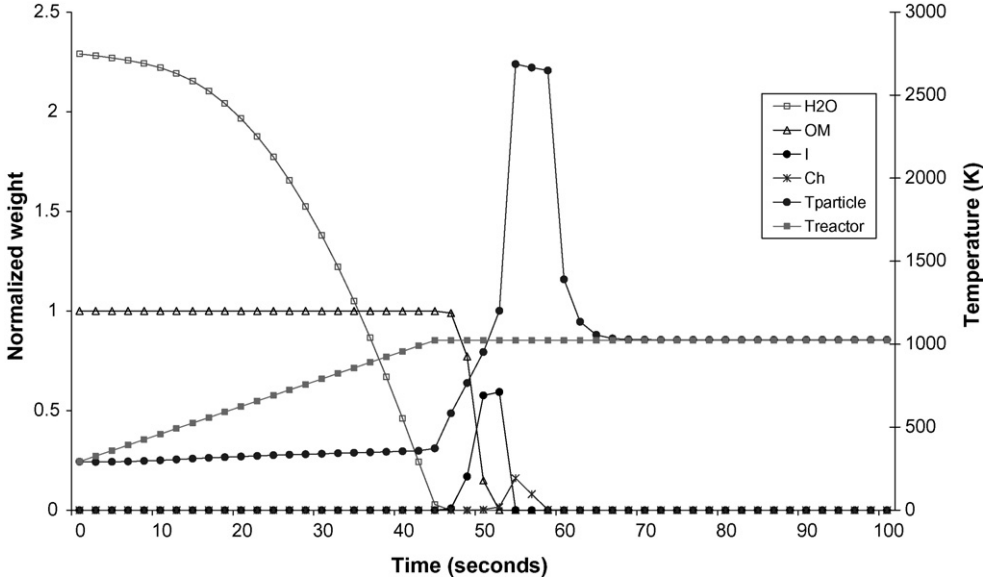

Fig. 4. Temperatures and incineration by-product mass fractions of sludge B2. Operating conditions: fluidized bed conditions 1000 K min^{-1} heating rate and $T_\infty = T_{reactor}$.

when compared to the TGA conditions with the high heating rate.

Finally and apart from the importance of transfers in fluidized bed (implying more efficient incineration), these simulations show that even if the incineration steps are more rapid, pyrolysis lasts a certain period of time. For our simulation, it goes on for during approximately 10 s in a whole process that lasts about 58 s (when drying is excluded, it even lasts more than 2/3 of the whole operation time). This shows that pyrolysis can no longer be considered instantaneous.

4. Conclusion

A numerical model has been elaborated in order to describe the incineration process of a single small particle of wet sewage sludge. An important characteristic of this model is that it includes drying of the incoming particle and heterogenous combustion of the pyrolysis residue, which is seldom taken into account when modeling thermal processing of sludge. Time dependencies of the particle radius, density, and temperature as well as incineration by-products were calculated. It was found that the mechanisms of sewage sludge incineration proceed at different rates and are interplaying mutually. After the entry of the sludge into the reactor, release of humidity and volatile substances into the surroundings occur almost immediately. The combustion is simultaneously started but, because of the very low value of the kinetic constant at this moment, heterogenoeus combustion does effectively influence the release of heat. It was found that operating conditions and especially the convective transfers influence greatly the process. Consequently, the need to accurately define the transfer conditions in order to be able to use TGA data in industrial issues was highlighted.

The ratio of primary to secondary volatiles was found to be greater in fluidized bed conditions and that thermogravimetric conditions favor the formation of rather light gases (secondary volatiles) to the detriment of tars. In fluidized conditions, simulations showed logically that heat and mass transfers are enhanced and consequently that incineration mecanisms are accelerated. Nevertheless, pyrolysis still takes nearly 2/3 of the whole process duration which justifies the fact that this step should be taken into account in the global model of fluidized bed combustors.

References

[1] S.C. Saxena, C.K. Jotshi, Fluidized-bed incineration of waste materials, Progr. Energy Comb. Sci. 20 (1994) 281–324.
[2] F. Scala, R. Chirone, Fluidized bed combustion of alternative solid fuels, Exp. Thermal Fluid Sci. 28 (2004) 691–699.
[3] J.J. Manya, J.L. Sanchez, J. Abrego, A. Gonzalo, J. Arauzo, Influence of gas residence time and air ratio on the air gasification of dried sewage sludge in a bubbling fluidised bed, Fuel 85 (2006) 2027–2033.
[4] R. Yan, D. Tee Liang, L. Tsen, Case studies—problem solving in fluidized bed waste fuel incineration, Energy Convers. Manage. 46 (2005) 1165–1178.
[5] F. Marias, J.R. Puiggali, G. Flamant, Modeling for simulation of fluidized-bed incineration process, AIChE J. 47 (2001) 1438–1460.
[6] B. Khiari, F. Marias, F. Zagrouba, J. Vaxelaire, Use of a transient model to simulate fluidized bed incineration of sewage sludge, J. Haz. Mat. 135 (2006) 200–209.
[7] J. Werther, T. Ogada, Sewage sludge combustion, Progr. Energy Comb. Sci. 25 (1999) 55–116.
[8] R. Font, A. Fullana, J.A. Conesa, F. Llavador, Analysis of the pyrolysis and combustion of different sewage sludges by TG, J. Anal. Appl. Pyrol. 58/59 (2001) 927–941.
[9] T. Ogada, J. Werther, Combustion characteristics of wet sludge in a fluidized bed, Fuel 75 (1996) 617–626.
[10] D.L. Urban, M.J. Antal Jr., Study of the kinetics of sewage sludge pyrolysis using DSC and TGA, Fuel 61 (1982) 799–806.
[11] J.A. Conesa, A. Marcilla, R. Moral, J. Moreno-Caselles, A. Perez-Espinosa, Evolution of gases in the primary pyrolysis of different sewage sludges, Thermochim. Acta 313 (1998) 63–73.
[12] S.A. Scott, J.S. Dennis, J.F. Davidson, A.N. Hayhurst, Thermogravimetric measurements of the kinetics of pyrolysis of dried sewage sludge, Fuel 85 (2006) 1248–1253.
[13] J. Nadziakiewicz, M. Kozio, Co-combustion of sludge with coal, Appl. Energy 75 (2003) 239–248.
[14] M. Inguanzo, A. Dominguez, J.A. Menendez, C.G. Blanco, J.J. Pis, On the pyrolysis of sewage sludge: the influence of pyrolysis conditions on solid, liquid and gas fractions, J. Anal. Appl. Pyrol. 63 (2002) 209–222.
[15] J.A. Menendez, A. Dominguez, M. Inguanzo, J.J. Pis, Microwave pyrolysis of sewage sludge: analysis of the gas fraction, J. Anal. Appl. Pyrol. 71 (2004) 657–667.
[16] W. Kaminsky, A.B. Kummer, Fluidized bed pyrolysis of digested sewage sludge, J. Anal. Appl. Pyrol. 16 (1989) 27–35.
[17] C.P. Chu, D.J. Lee, C.Y. Chang, Thermal pyrolysis characteristics of polymer flocculated waste activated sludge, Water Res. 35 (2001) 49–56.
[18] C. Chao, H. Chiang, C. Chen, Pyrolytic kinetics of sludge from a petrochemical factory wastewater treatment plant—a transition state theory approach, Chemosphere 49 (2002) 431–437.
[19] L.F. Calvo, M. Otero, B.M. Jenkins, A.I. Garcia, A. Moran, Heating process characteristics and kinetics of sewage sludge in different atmospheres, Thermochim. Acta 409 (2004) 127–135.
[20] R. Font, A. Fullana, J. Conesa, Kinetic models for the pyrolysis and combustion of two types of sewage sludge, J. Anal. Appl. Pyrol. 74 (2005) 429–438.
[21] M.B. Folgueras, R. Maria-Diaz, J. Xiberta, Pyrolysis of blends of different types of sewage sludge with one bituminous coal, Energy 30 (2005) 1079–1091.
[22] X. Chen, S. Jeyaseelan, Study of sewage sludge pyrolysis mechanism and mathematical modeling, J. Env. Eng. 127 (2001) 585–593.
[23] R. Dumpelmann, W. Richarz, M.R. Stammbach, Kinetic studies of the pyrolysis of sewage sludge by TGA and comparison with fluidized beds, Can. J. Chem. Eng. 69 (1991) 953–963.
[24] E. Biagini, F. Lippi, L. Petarca, L. Tognotti, Devolatilization rate of biomasses and coal–biomass blends: an experimental investigation, Fuel 81 (2002) 1041–1050.
[25] D. Rong, M. Horio, DEM simulation of char combustion in a fluidized bed, in: Proceedings of the Second International Conference on CFD in the Minerals and Process Industries. CSIRO, Melbourne, Australia, December 6–8, 1999.
[26] J. Vaxelaire, J.R. Puiggali, Analysis of the drying of residual sludge: from the experiment to the simulation of belt dryer, Drying Technol. 20 (2002) 989–1008.
[27] J. Vaxelaire, Moisture sorption characteristics of waste activated sludge, J. Chem. Technol. Biotechnol. 76 (2001) 377–382.
[28] I. Tosun, Modeling in Transport Phenomena, 1st ed., Elsevier, Amsterdam, 2002.
[29] R.C. Reid, J.M. Prausnitz, B.E. Poling, The Properties of Gases and Liquids, 4th ed., McGraw-Hill, New York, 1987.
[30] S. Sriramulu, S. Sane, P. Agarwal, T. Mathews, Mathematical modelling of fluidized bed combustion. 1. Combustion of carbon in bubbling beds, Fuel 75 (1996) 1351–1362.

[31] W. Prins, Fluidized bed combustion of a single carbon particle, PhD Thesis, University of Twente, 1987.
[32] V. Thonglip, N. Hiquily, C. Laguérie, Vitesse minimale de fluidisation et expansion des couches fluidisées par un gaz, Powder Technol. 38 (1984) 233–253.
[33] J.M. Bongiovanni, Traitement des boues résiduaires par association en série d'une déshydratation mécanique et d'un séchage thermique, PhD Thesis, Université de Pau et des Pays de l'Adour, France, 1998.
[34] A. Genin, Modélisation des phénomènes de transport dans une thermobalance, PhD Thesis, Université Jean Monnet de Saint-Etienne, France, 2004.